

atom-atom intermolecular distances. Index i in the summation runs over all atoms of one molecule (chosen as a reference molecule, and index j , over the atoms of the surrounding molecules distributed according to crystal symmetry. A cutoff of 15 Å has been adopted in our calculations. The values of the coefficients A , B , and C used in this work have been taken from the literature^{11b} and discussed in previous papers.¹² The results of PPE calculations are used to select the first-neighboring molecules (FNM) among the molecules surrounding the one chosen as reference (RM) on the basis of the contribution to PPE.¹² It should be stressed that this procedure is used only as a convenient means to investigate the molecular environment within the crystalline lattice without pretensions of obtaining "true" (or even

approximate) crystal potential energy values.

All calculations were carried out with the aid of the computer program OPEC.¹³ SCHAKAL88¹⁴ was used for the graphical representation of the results.

Acknowledgment. We thank the SERC and British Petroleum (P.J.D.) for financial assistance. Financial support by the MURST (Italy) is also acknowledged; D.B., F.G., and B.F.G.J. acknowledge NATO for a travel grant.

Supplementary Material Available: For all species discussed herein, tables of anisotropic thermal parameters, fractional atomic coordinates and thermal parameters, fractional atomic coordinates for the hydrogen atoms, and complete bonds and angles (33 pages). Ordering information is given on any current masthead page.

OM920244V

(11) (a) Kitaigorodsky, A. I. *Molecular Crystal and Molecules*; Academic Press: New York, 1973. (b) Pertsin, A. J.; Kitaigorodsky, A. I. *The Atom-Atom Potential Method*; Springer-Verlag: Berlin, 1987. (c) Gavezzotti, A.; Simonetta, M. *Chem. Rev.* 1981, 82, 1. (d) Mirsky, K. *Computing in Crystallography, Proceedings of the International Summer School on Crystallographic Computing*; Delf University Press: Twente, The Netherlands, 1978; p 169.

(12) (a) Braga, D.; Grepioni, F.; Sabatino, P. *J. Chem. Soc., Dalton Trans.* 1990, 3137. (b) Braga, D.; Grepioni, F. *Organometallics* 1991, 10, 1254. (c) Braga, D.; Grepioni, F.; *Organometallics* 1991, 10, 2563. (d) Braga, D.; Grepioni, F. *Organometallics* 1992, 11, 711.

(13) Gavezzotti, A. OPEC. *Organic Packing Potential Energy Calculations*; University of Milano: Milano, Italy. See also: Gavezzotti, A. *J. Am. Chem. Soc.* 1983, 105, 5220.

(14) Keller, E. SCHAKAL88. *Graphical Representation of Molecular Models*; University of Freiburg: Freiburg, FRG.

Alkyne Addition to the Semlinterstitial Boron Atom in Homometallic and Heterometallic Butterfly Clusters: Molecular and Electronic Structures of $\text{HRu}_4(\text{CO})_{12}\text{BHC}(\text{Ph})\text{CPhH}$ and $\text{H}(\text{CpW})\text{Ru}_3(\text{CO})_{11}\text{BC}(\text{Ph})\text{CPhH}$

Catherine E. Housecroft,* James S. Humphrey, Ann K. Keep, Dorn M. Matthews, and Nicola J. Seed

University Chemical Laboratory, Lensfield Road, Cambridge CB2 1EW, U.K.

Brian S. Haggerty and Arnold L. Rheingold*

Department of Chemistry, University of Delaware, Newark, Delaware 19716

Received July 13, 1992

The clusters $\text{HRu}_4(\text{CO})_{12}\text{BH}_2$ and $\text{H}(\text{CpW})\text{Ru}_3(\text{CO})_{11}\text{BH}$ both undergo alkyne coupling reactions with diphenylacetylene to form $\text{HRu}_4(\text{CO})_{12}\text{BHC}(\text{Ph})\text{CPhH}$, **1**, and $\text{H}(\text{CpW})\text{Ru}_3(\text{CO})_{11}\text{BC}(\text{Ph})\text{CPhH}$, **2**, respectively. In each case one Ru-H-B bridging hydrogen atom is transferred to the alkyne and a B-C bond is formed. The molecular structures of the two products have been determined by single-crystal X-ray diffraction, and a comparison of the two structures shows that the introduction of the heterometal atom into the butterfly framework of the precursor has a significant influence upon the nature of the product obtained. **1**: monoclinic, $P2_1/c$; $a = 9.758$ (2), $b = 36.653$ (8), $c = 17.131$ (4) Å; $\beta = 101.92$ (2)°; $V = 5996$ (3) Å³; $Z = 8$; $R(F) = 5.56\%$. **2**: monoclinic, $P2_1/n$; $a = 14.324$ (4), $b = 13.983$ (3), $c = 16.618$ (3) Å; $\beta = 108.47$ (2)°; $V = 3157$ (2) Å³; $Z = 4$; $R(F) = 4.35\%$. The four ruthenium atoms in **1** define a spiked triangle; the boron atom interacts with all four metal atoms, and the alkyne resides in a position such that it bonds to the boron atom and two ruthenium atoms including that of the spike. In contrast, the tungsten and three ruthenium atoms in **2** retain the butterfly skeleton of the precursor and the alkyne interacts with the boron atom and one ruthenium atom only. Differences in bonding with respect to boron-alkyne coupling in **1** and **2** are addressed by use of the Fenske-Hall molecular orbital method, and appropriate electron counting schemes for the two compounds are assessed in the light of the results of the MO calculations.

In a preliminary publication¹ we reported that the reaction of diphenylacetylene with the tetraruthenaborane $\text{HRu}_4(\text{CO})_{12}\text{BH}_2$ resulted in insertion of the alkyne into the butterfly framework of $\text{HRu}_4(\text{CO})_{12}\text{BH}_2$ with concomitant B-C bond formation, B-H bond activation, and

Ru_4 -skeletal opening (Figure 1a). This result was in contrast to that observed for the reaction of $\text{PhC}\equiv\text{CPh}$ with $\text{H}_2\text{Ru}_4(\text{CO})_{12}\text{C}$ (which exists as the mixture of isomers $\text{H}_2\text{Ru}_4(\text{CO})_{12}\text{C}$ and $\text{HRu}_4(\text{CO})_{12}\text{CH}$)² or $[\text{Ru}_4(\text{CO})_{12}\text{N}]^{-3}$

(1) Chipperfield, A. K.; Haggerty, B. S.; Housecroft, C. E.; Rheingold, A. L. *J. Chem. Soc., Chem. Commun.* 1990, 1174.

(2) Dutton, T.; Johnson, B. F. G.; Lewis, J.; Owen, S. M.; Raithby, P. *R. J. Chem. Soc., Chem. Commun.* 1988, 1423.

(3) Blohm, M.; Gladfelter, W. L. *Organometallics* 1986, 5, 1049.

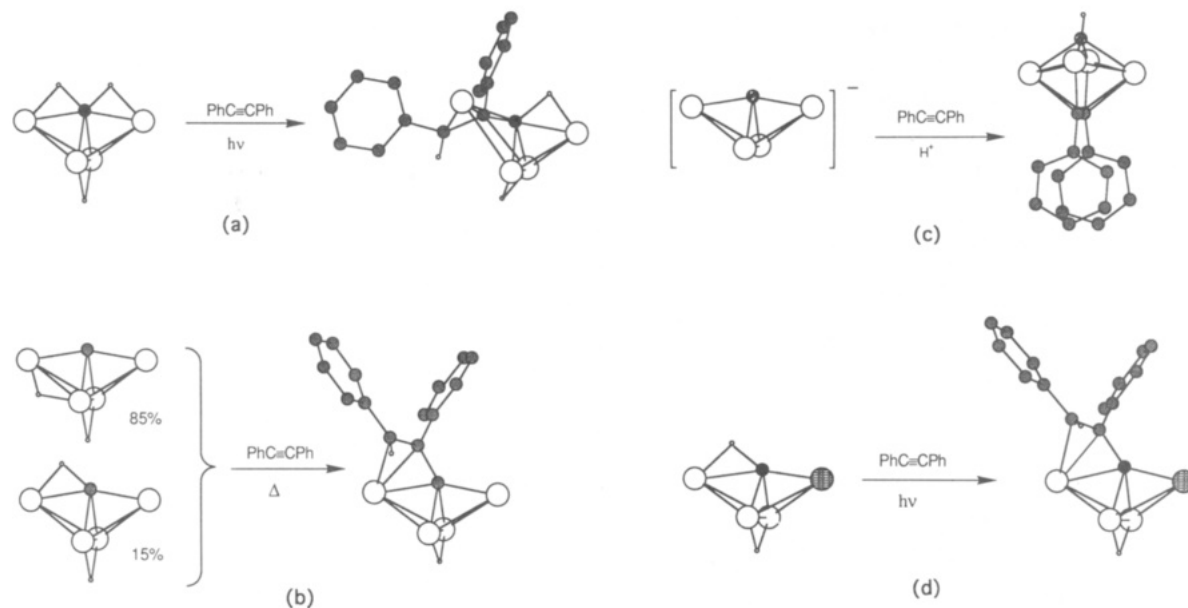


Figure 1. Schematic representations of the reactions of PhC≡CPh with (a) $\text{HRu}_4(\text{CO})_{12}\text{BH}_2$, (b) $\text{H}_2\text{Ru}_4(\text{CO})_{12}\text{C}$, (c) $[\text{Ru}_4(\text{CO})_{12}\text{N}]^-$, and (d) $\text{H}(\text{CpW})\text{Ru}_3(\text{CO})_{11}\text{BH}$.

(Figures 1b and 1c), both of which are isoelectronic with $\text{HRu}_4(\text{CO})_{12}\text{BH}_2$.

The introduction of a heterometal atom into a butterfly M_4E framework (M = transition metal and E = first-row p-block element) will perturb the electronic structure of the skeleton. This may be slight as in the case of the change from $[\text{Ru}_4(\text{CO})_{12}\text{N}]^-$ to $[\text{Ru}_3\text{Fe}(\text{CO})_{12}\text{N}]^{-4}$ or may, for example, influence the site of cluster protonation.⁵ Studies of the reactivity of butterfly clusters containing a semiinterstitial boron atom are still few,⁶ and only recently have examples of heterometallic clusters with the $\text{M}_3\text{M}'\text{B}$ -butterfly core been prepared.^{7,8} It was therefore of interest to investigate whether the reaction of an acetylene with a heterometallic butterfly boride cluster paralleled or not the analogous reaction with an isoelectronic⁹ homometallic cluster. We now report in full the reaction of $\text{HRu}_4(\text{CO})_{12}\text{BH}_2$ with PhC≡CPh and compare it with the reaction of the heterometallic butterfly cluster $\text{H}(\text{CpW})\text{Ru}_3(\text{CO})_{11}\text{BH}$ with the same alkyne.

Experimental Section

General Data. FT-NMR spectra were recorded on a Bruker WM 250 or AM 400 spectrometer. ^1H NMR shifts are reported with respect to δ 0 for Me_4Si ; ^{11}B NMR shifts, with respect to δ 0 for $\text{F}_3\text{B-OEt}_2$. All downfield chemical shifts are positive. Infrared spectra were recorded on a Perkin-Elmer FT 1710 spectrophotometer. FAB mass spectra were recorded on a Kratos MS 50TC, MS 902, or MS 890 instrument.

All reactions were carried out under argon by using standard Schlenk techniques. Solvents were dried over suitable reagents and freshly distilled under N_2 before use. Separations were carried out by thin-layer plate chromatography with Kieselgel 60-PF-254 (Merck). Diphenylacetylene (Aldrich) was used as received. $\text{HRu}_4(\text{CO})_{12}\text{BH}_2$ and $\text{H}(\text{CpW})\text{Ru}_3(\text{CO})_{11}\text{BH}$ were prepared by

published methods.^{8,10} Photolysis experiments used a mercury high-pressure lamp (Aldrich).

Reaction of $\text{HRu}_4(\text{CO})_{12}\text{BH}_2$ with PhC≡CPh. In a typical reaction, $\text{HRu}_4(\text{CO})_{12}\text{BH}_2$ (52.8 mg, 0.07 mmol) and PhC≡CPh (60.5 mg, 0.34 mmol) were dissolved in CH_2Cl_2 (2 mL) or CDCl_3 (2 mL) in a quartz tube. The solution was photolyzed for 16 h during which time the color of the solution changed from yellow to orange-red. Solvent was removed in vacuo, and the products were separated by TLC eluting with hexane. The first band was visible under UV radiation and was not collected. The second and third fractions were identified as $\text{H}_4\text{Ru}_4(\text{CO})_{12}$ and unreacted $\text{HRu}_4(\text{CO})_{12}\text{BH}_2$,^{10,11} respectively. The fourth fraction (orange, yield \approx 35%) was $\text{HRu}_4(\text{CO})_{12}\text{BHC}(\text{Ph})\text{CPhH}$, **1**. The fifth band to be eluted was red-orange in color and was identified from infrared and mass spectral data as consisting of a mixture of isomers of $\text{Ru}_3(\text{CO})_8(\text{PhCCPh})_2$.¹²⁻¹⁴ Two further fractions (brown and red, respectively) were collected in minor amounts but have eluded complete characterization. The yield of **1** may be increased to about 60% by altering the molar ratio of $\text{HRu}_4(\text{CO})_{12}\text{BH}_2$:PhC≡CPh to 1:3 and extending the period of photolysis to 22 h. Compound **1**: 250-MHz ^1H NMR (CDCl_3 , 298 K) δ 7.4–7.0 (m, Ph), 5.04 (s, CH), -7.3 (br, Ru-H-B), -19.06 (s, Ru-H-Ru); 128-MHz ^{11}B NMR (CDCl_3 , 298 K) δ +93.7 (d, J_{BH} 40 Hz); IR (hexane, cm^{-1}) ν_{CO} 2098 w, 2073 vs, 2060 s, 2049 vs, 2027 m, 2018 m, 2012 w, 1997 w; FAB-MS in 3-NBA matrix, m/z 934 (P^+) with 12 CO losses observed (observed isotopic pattern agrees with that simulated for $\text{C}_{26}\text{H}_{13}\text{BO}_{12}\text{Ru}_4$).

Reaction of $\text{H}(\text{CpW})\text{Ru}_3(\text{CO})_{11}\text{BH}$ with PhC≡CPh. In a typical reaction, $\text{H}(\text{CpW})\text{Ru}_3(\text{CO})_{11}\text{BH}$ (8.7 mg, 0.01 mmol) and PhC≡CPh (8.9 g, 0.05 mmol) were dissolved in CH_2Cl_2 (1 mL) in a quartz tube. The solution was photolyzed for 16 h during which time the color of the solution changed from pink-red to pale brown. Solvent was removed in vacuo, and the products were separated by TLC eluting with hexane. The first band was visible under UV radiation and was not collected. The second fraction (pale orange, yield \approx 20%) was unreacted $\text{H}(\text{CpW})\text{Ru}_3(\text{CO})_{11}\text{BH}$. The third fraction (dark orange, yield \approx 75%) was identified as a mixture of isomers (see text) of $\text{H}(\text{CpW})\text{Ru}_3(\text{CO})_{11}\text{BC}(\text{Ph})\text{CPhH}$,

(4) Harris, S.; Blohm, M. L.; Gladfelter, W. L. *Inorg. Chem.* **1989**, *28*, 2290.

(5) Hriljac, J. A.; Harris, S.; Shriver, D. F. *Inorg. Chem.* **1988**, *27*, 816.

(6) Housecroft, C. E. *Adv. Organomet. Chem.* **1991**, *33*, 1.

(7) Draper, S. M.; Housecroft, C. E.; Keep, A. K.; Matthews, D. M.; Song, X.; Rheingold, A. L. *J. Organomet. Chem.* **1992**, *423*, 241.

(8) Housecroft, C. E.; Matthews, D. M.; Rheingold, A. L.; Song, X. *J. Chem. Soc., Dalton Trans.* **1992**, 2855.

(9) The term isoelectronic is used here with reference to the valence electrons only. Thus, both $\text{HRu}_4(\text{CO})_{12}\text{BH}_2$ and $\text{H}(\text{CpW})\text{Ru}_3(\text{CO})_{11}\text{BH}$ are isoelectronic 62-electron butterfly clusters.

(10) Chipperfield, A. K.; Housecroft, C. E.; Rheingold, A. L. *Organometallics* **1990**, *9*, 681.

(11) Hong, F.-E.; Coffy, T. J.; McCarthy, D. A.; Shore, S. G. *Inorg. Chem.* **1989**, *28*, 3284.

(12) Cetini, G.; Gambino, O.; Sappa, E.; Valle, M. *J. Organomet. Chem.* **1969**, *17*, 437.

(13) Rivomanana, S.; Lavigne, G.; Lugan, N.; Bonnet, J.-J.; Yanez, R.; Mathieu, R. *J. Am. Chem. Soc.* **1989**, *111*, 8959.

(14) Rivomanana, S.; Lavigne, G.; Lugan, N.; Bonnet, J.-J. *Organometallics* **1991**, *10*, 2285.

Table I. Crystal Data for Compounds 1 and 2

	1	2
(a) Crystal Parameters		
formula	C ₂₆ H ₁₃ BO ₁₂ Ru ₄	C ₃₀ H ₁₆ BO ₁₁ Ru ₃ W
fw	932.47	1050.32
cryst system	monoclinic	monoclinic
space group	P2 ₁ /c	P2 ₁ /n
a, Å	9.758 (2)	14.324 (4)
b, Å	36.653 (8)	13.983 (3)
c, Å	17.131 (4)	16.618 (3)
β, deg	101.92 (2)	108.47 (2)
V, Å ³	5996 (3)	3157 (2)
Z	8	4
cryst dims, mm	0.32 × 0.41 × 0.56	0.31 × 0.32 × 0.36
cryst color	orange-red	black
D(calc), g cm ⁻³	2.066	2.210
μ(Mo Kα), cm ⁻¹	19.99	50.98
temp, K	294	292
T(max)/T(min)	1.47	1.22
(b) Data Collection		
diffractometer	Nicolet R3m	Siemens P4
monochromator	graphite	graphite
radiation	Mo Kα	Mo Kα
2θ scan range, deg	4–52	4–54
no. of data colld	±h, ±k, ±l	±h, ±k, ±l
no. of rflns colld	12 843	7423
no. of indpt rflns	11 764	6885
R(merge), %	0.76	1.93
no. of indpt obsd rflns	7001 (n = 5)	5402 (n = 4)
F _o ≥ nσ(F _o)		
std rflns	3 std/197 rflns	3 std/197 rflns
var in stds, %	<1	<1
(c) Refinement		
R(F), %	5.56	4.35
R _w (F), %	5.53	5.31
Δ/σ(max)	0.10	0.02
Δ(ρ), e Å ⁻³	1.21	2.61
N _o /N _v	9.63	12.8
GOF	1.20	1.27

2. 2: 250-MHz ¹H NMR (CDCl₃, 298 K) δ 7.3–6.8 (m, Ph), 5.98 (s, isomer I, CH), 5.53 (s, isomer II, CH), 5.29 (s, Cp), -20.5 (s, Ru-H-Ru); 128-MHz ¹¹B NMR (CDCl₃, 298 K) δ +125.0 (s); IR (hexane, cm⁻¹) ν_{CO} 2083 w, 2076 m, 2047 vs, 2038 s, 2009 s, 2000 w, 1986 m, 1978 m, 1967 m, 1904 m; FAB-MS in 3-NBA matrix, m/z 1052 (P⁺) with 11 CO losses observed (observed isotopic pattern agrees with that simulated for C₃₀H₁₇BO₁₁Ru₃W).

Crystal Structure Determinations. Crystallographic data for 1 and 2 are combined in Table I. The experimental methods used were essentially similar. Specimens were mounted on glass fibers, and 2/m Laue symmetry was determined by photographic methods. The systematic absences in the data uniquely determined the assigned space groups. The data sets were corrected for absorption effects by semiempirical methods using an ellipsoidal model. The structures were solved by direct methods. All non-hydrogen atoms were refined using anisotropic thermal parameters, and hydrogen atoms were treated as idealized contributions, except for the hydrogen atoms on B and C(13) in 1 which were ignored. Phenyl rings were constrained to rigid, planar hexagons. All calculations used PC versions of SHELXTL software.

Molecular Orbital Calculations. Fenske-Hall calculations¹⁵ were carried out on the model compounds HRu₄(CO)₁₂BHCH₂ and H(CpMo)Ru₃(CO)₁₁BCHCH₂ in terms of the orbital interactions between the fragments [HRu₄(CO)₁₂BH]⁻ and [C₂H₃]⁺ or [H(CpMo)Ru₃(CO)₁₁B]⁻ and [C₂H₃]⁺, respectively. The geometry of each molecule was taken directly from that crystallographically determined for HRu₄(CO)₁₂BHC(Ph)CPhH and H(CpW)Ru₃(CO)₁₁BC(Ph)CPhH but with a molybdenum atom replacing the tungsten atom and with hydrogen atoms replacing the phenyl substituents (C-H = 1.0 Å). The calculations employed single-ζ Slater functions for the 1s and 2s orbitals of B, C, and O. Exponents were obtained by curve fitting the double-ζ functions of

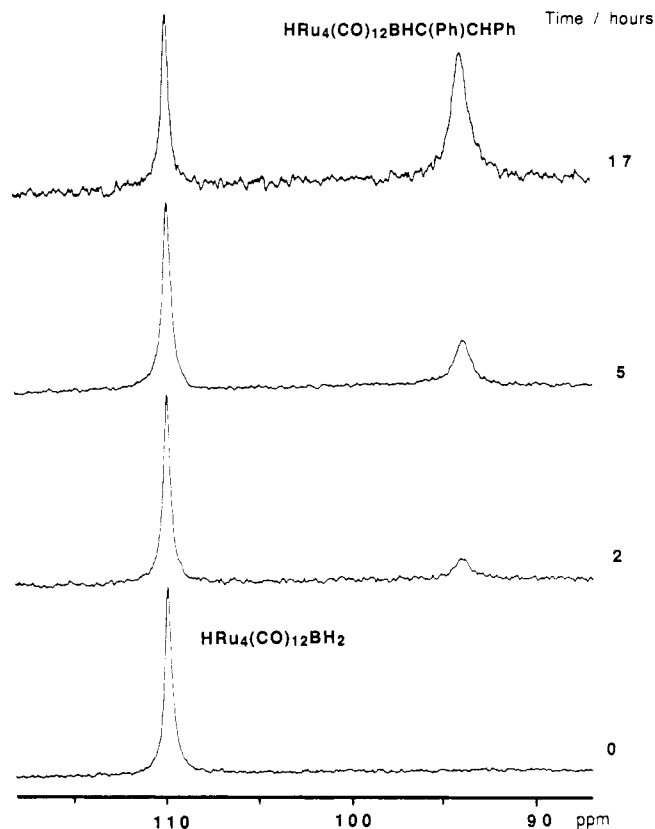


Figure 2. ¹¹B{¹H} NMR spectroscopic monitoring of the photolysis of HRu₄(CO)₁₂BH₂ with PhC≡CPh in CDCl₃ over a period of 17 h.

Clementi¹⁶ while maintaining orthogonal functions. Double-ζ functions were used directly for the 2p orbitals. An exponent of 1.16 was used for H. The Ru and Mo atoms¹⁷ were augmented by 5s and 5p functions with exponents of 2.20.

Results and Discussion

Reaction of Diphenylacetylene with HRu₄(CO)₁₂BH₂. Upon photolysis in dichloromethane solution, HRu₄(CO)₁₂BH₂ reacts with PhC≡CPh to yield HRu₄(CO)₁₂BHC(Ph)CPhH, 1, as the main product (Figure 1a). The reaction has been monitored by use of ¹¹B{¹H} NMR spectroscopy as shown in Figure 2. No other boron-containing products are observed during a reaction period of 17 h. The ¹¹B NMR resonance for HRu₄(CO)₁₂BH₂ is a triplet (*J*_{BH} = 70 Hz) at δ +109.9.^{10,11} As this signal decays, a new signal at δ +93.7 grows in; this appears as a doublet, with *J*_{BH} = 40 Hz. The nature of the resonance and the magnitude of the ¹¹B-¹H coupling indicates the retention of one B-H-Ru bridging proton in the product. This is confirmed in the ¹H NMR spectrum of 1 in which a broad signal at δ -7.3, characteristic of an Ru-H-B interaction, is observed. The appearance in the ¹H NMR spectrum of 1 of a singlet at δ +5.04 suggests that the cluster-bound hydrogen atom has been transferred to the alkyne rendering the latter olefinic in nature.

The butterfly framework of HRu₄(CO)₁₂BH₂ possesses a hydride ligand bridging the Ru_{hinge}-Ru_{hinge} edge. In the ¹H NMR spectrum, this is characterized by a sharp singlet at δ -21.18.^{10,11} We have noted that in compounds which retain the butterfly {(μ-H)Ru₄B} core, little variation in the chemical shift of the resonance assigned to the hinge

(16) Clementi, E. *J. Chem. Phys.* 1964, 40, 1944.

(17) Richardson, J. W.; Blackman, M. J.; Ranochak, J. F. *J. Chem. Phys.* 1973, 58, 3010.

(15) Hall, M. B.; Fenske, R. F. *Inorg. Chem.* 1972, 11, 768.

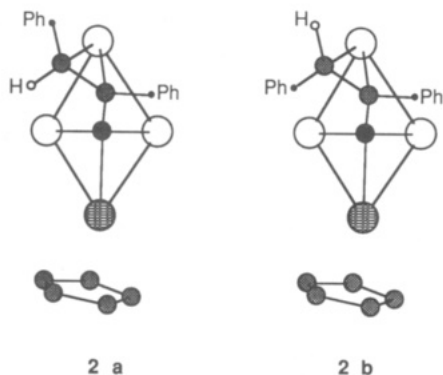


Figure 3. Proposed structures of the two isomers of compound 2. The carbonyl ligands have been omitted for clarity. Structure 2a has been confirmed crystallographically.

bridging hydride ligand is apparent.^{6,18} Thus, the appearance of a hydride resonance at $\delta -19.06$ in 1 signifies that the butterfly framework has been perturbed upon reaction with the alkyne. This has been confirmed crystallographically.

The formation of 1 from $\text{HRu}_4(\text{CO})_{12}\text{BH}_2$ competes with a reaction route which destroys the metallaborane butterfly cluster. The two isomers of $\text{Ru}_3(\text{CO})_8(\text{PhCCPh})_2$ which have previously been reported¹²⁻¹⁴ were both identified as products of the photolysis of $\text{HRu}_4(\text{CO})_{12}\text{BH}_2$ with $\text{PhC}\equiv\text{CPh}$.

Reaction of Diphenylacetylene with $\text{H}(\text{CpW})\text{Ru}_3(\text{CO})_{11}\text{BH}$. The replacement of a wing-tip $\{\text{HRu}(\text{CO})_3\}$ fragment in $\text{HRu}_4(\text{CO})_{12}\text{BH}_2$ by an electronically equivalent $\{\text{CpW}(\text{CO})_2\}$ fragment has the effect of increasing the boridic nature of the semiinterstitial boron atom in the tetrametal butterfly. In $\text{H}(\text{CpW})\text{Ru}_3(\text{CO})_{11}\text{BH}$ the boron atom is bonded directly to three metal atoms and indirectly via an Ru-H-B bridge to the fourth metal atom. The hinge of the butterfly is bridged by a hydride ligand characterized in the ^1H NMR spectrum by a signal at $\delta -20.4$; the Ru-H-B bridging hydrogen atom gives rise to a broad signal at $\delta -6.6$.⁹ In dichloromethane, $\text{H}(\text{CpW})\text{Ru}_3(\text{CO})_{11}\text{BH}$ reacts with $\text{PhC}\equiv\text{CPh}$ to give $\text{H}(\text{CpW})\text{Ru}_3(\text{CO})_{11}\text{BC}(\text{Ph})\text{CPhH}$, 2, in high yield (Figure 1d). Appreciable differences exist between the product type obtained in this reaction and in the reaction of $\text{HRu}_4(\text{C-O})_{12}\text{BH}_2$. Compound 2 is characterized in the ^{11}B NMR spectrum by a singlet at $\delta +125.0$; this compares to a doublet ($J_{\text{BH}} = 65$ Hz) for the starting cluster $\text{H}(\text{CpW})\text{Ru}_3(\text{CO})_{11}\text{BH}$ indicating that the original Ru-H-B bridging hydrogen atom has been replaced by a direct Ru-B interaction. The loss of the Ru-H-B bridge is confirmed in the high-field part of the ^1H NMR spectrum of 2 where only a singlet at $\delta -20.5$ is observed. The similarity between this and the hydridic shift for the starting material implies that the butterfly framework of $\text{H}(\text{CpW})\text{Ru}_3(\text{CO})_{11}\text{BH}$ ⁸ is not appreciably perturbed during the reaction.

The gain of a hydrogen atom by the alkyne molecule is supported by the appearance of signals due to an olefinic CH group. The appearance of two such signals ($\delta +5.53$ and $+5.98$ in an approximate ratio 1:1) indicates the formation of two isomers of 2. This is supported by the appearance of two signals ($\delta +93.2$ and $+95.2$) in the $^{13}\text{C}\{^1\text{H}\}$ NMR spectrum which collapse upon proton coupling and may be assigned as CH-carbon atoms from results of an APT (attached proton test) experiment. We propose that

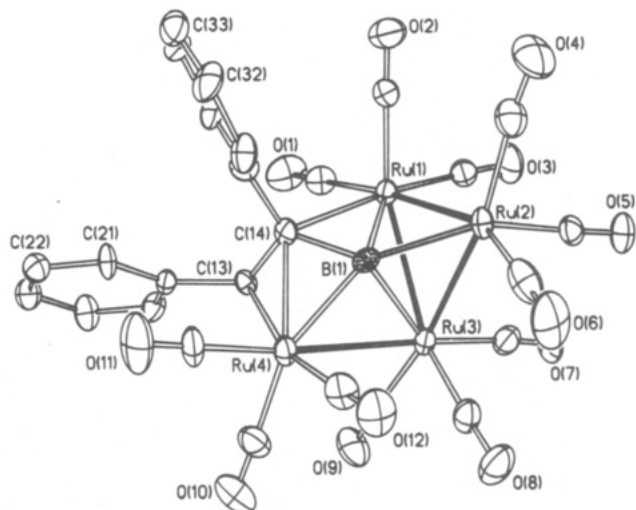


Figure 4. Molecular structure of $\text{HRu}_4(\text{CO})_{12}\text{BHC}(\text{Ph})\text{CPh}$, 1. Cluster hydrogen atoms were not located.

the two isomers of 2 are both related (see structural determination presented below) and differ only in the orientation of the $\{\text{PhCCHPh}\}$ group with respect to the Ru_3WB framework (Figure 3).

Molecular Structure of 1. The molecular structure of 1 is illustrated in Figure 4, and selected bond distances and angles are given in Table III.¹⁹ The cluster exhibits an unusual spiked triangular tetraruthenium framework with the boron atom within bonding contact of all four metal atoms. Thus, the butterfly framework of $\text{HRu}_4(\text{C-O})_{12}\text{BH}_2$ is opened up as reaction with the alkyne occurs; $\text{Ru}(1)\cdots\text{Ru}(4) = 4.007$ (1) Å. This arrangement of one boron and four metal atoms is unprecedented. Ru-B distances range from 2.152 (13) to 2.236 (14) Å, the longest edge being associated with the bridging atom C(14). Interestingly, and in contrast to the features noted in the structure of 2 described below, the edge $\text{Ru}(4)\text{-B}(1)$ which is bridged by the organic fragment is not very much longer than the wing tip-ruthenium-boron atom edge in $\text{HRu}_4(\text{CO})_{12}\text{BH}_2$ ²⁰ from which it originated; $\text{Ru}(4)\text{-B}(1) = 2.152$ (13) Å compared to distances for $\text{Ru}_{\text{wing-B}}$ in $\text{HRu}_4(\text{C-O})_{12}\text{BH}_2$ of 2.111 (6) and 2.106 (6) Å.²⁰

The organic fragment which originates from the $\text{PhC}\equiv\text{CPh}$ molecule is bonded both to the boron atom and to two ruthenium atoms in 1. Atoms C(13) and C(14) are approximately equidistant from atom Ru(4), and the mode of attachment may be considered in terms of an alkene-like π -interaction; this is discussed in detail below. Atom C(13) carries a terminal hydrogen atom; although this was not directly located crystallographically, its presence may be inferred from (i) the orientation of the phenyl substituent attached to C(13) with respect to atoms C(14) and Ru(4) and (ii) the observation of an olefinic proton in the ^1H NMR spectrum of 1. The distance of 1.466 (14) Å for the bond C(13)-C(14) supports the premise of an olefinic unit, bound in a π -fashion to atom Ru(4). However, the environment around C(14) is unusual; the atom carries one phenyl substituent, is involved in the π -interaction to atoms C(13) and Ru(4), and also interacts with both atoms Ru(1) and B(1). The distance of 1.612 (17) Å for B(1)-C(14) is at one end of the range (1.58-1.62 Å) expected for

(19) There are two independent molecules in the unit cell. Parameters given in Table III are for both molecules A and B although the discussion centers only on molecule A since there are no chemically significant differences between the independent molecules. Full data for both molecules are available in the supplementary data.

(20) Hong, F.-E.; McCarthy, D. A.; White, J. P., III; Cottrell, C. E.; Shore, S. G. *Inorg. Chem.* 1990, 29, 2874.

(18) Draper, S. M.; Housecroft, C. E.; Rees, J. E.; Shongwe, M. S.; Haggerty, B. S.; Rheingold, A. L. *Organometallics* 1992, 11, 2356.

Table II. Atomic Coordinates ($\times 10^4$) and Isotropic Thermal Parameters ($\text{\AA}^2 \times 10^3$) for 1

	x	y	z	U^a		x	y	z	U^a
Ru(1)	1465.1 (10)	939.8 (2)	2427.3 (4)	29.3 (3)	C(10)	-3395 (13)	1544 (4)	2647 (8)	53 (5)
Ru(2)	1083.6 (10)	574.7 (3)	3798.5 (6)	33.9 (3)	C(11)	-1517 (14)	1914 (3)	3773 (8)	48 (5)
Ru(3)	-1318.7 (10)	714.1 (2)	2619.1 (6)	30.3 (3)	C(12)	-1990 (14)	1236 (4)	4203 (7)	47 (5)
Ru(4)	-1571.0 (10)	1453.9 (2)	3252.0 (6)	32.8 (3)	C(13)	-527 (10)	1624 (3)	2304 (6)	27 (4)
Ru(1')	5968.3 (9)	1352.2 (2)	9009.4 (5)	29.4 (3)	C(14)	561 (11)	1473 (3)	2942 (7)	31 (4)
Ru(2')	5089.1 (10)	628.1 (2)	8968.7 (6)	34.8 (3)	C(21)	-321 (8)	2328 (2)	2486 (3)	40 (4)
Ru(3')	6458.4 (10)	855.9 (3)	7753.1 (6)	32.2 (1)	C(22)	-592	2676	2157	47 (5)
Ru(4')	3806.2 (10)	1148.0 (2)	6800.0 (5)	31.3 (3)	C(23)	-1220	2715	1353	49 (5)
B(1)	189 (13)	1093 (4)	3321 (7)	30 (4)	C(24)	-1576	2406	877	46 (5)
B(1')	4498 (13)	1046 (3)	8048 (8)	47 (5)	C(25)	-1305	2059	1206	40 (4)
O(1)	1650 (11)	1385 (3)	933 (6)	76 (5)	C(26)	-678	2020	2010	28 (4)
O(2)	4447 (10)	1053 (3)	3338 (7)	76 (5)	C(31)	1956 (8)	1758 (2)	4224 (4)	42 (5)
O(3)	2266 (11)	224 (3)	1776 (6)	68 (4)	C(32)	3100	1958	4629	54 (5)
O(4)	4085 (11)	474 (3)	4762 (7)	92 (5)	C(33)	4019	2120	4208	54 (5)
O(5)	1104 (10)	-210 (2)	3232 (5)	58 (4)	C(34)	3793	2082	3381	44 (5)
O(6)	-372 (13)	394 (3)	5163 (6)	87 (5)	C(35)	2648	1882	2975	37 (4)
O(7)	-1305 (10)	-39 (2)	1839 (6)	61 (4)	C(36)	1730	1720	3397	36 (4)
O(8)	-3191 (11)	438 (3)	3698 (6)	72 (5)	C(1')	6514 (13)	1852 (3)	8916 (8)	48 (5)
O(9)	-3740 (11)	953 (3)	1324 (6)	72 (4)	C(2')	4867 (12)	1423 (3)	9808 (7)	39 (4)
O(10)	-4473 (10)	1603 (3)	2251 (6)	77 (5)	C(3')	7552 (13)	1228 (3)	9774 (7)	44 (5)
O(11)	-1463 (13)	2176 (3)	4130 (6)	89 (5)	C(4')	3972 (15)	613 (4)	9759 (8)	54 (5)
O(12)	-2169 (11)	1119 (3)	4788 (6)	68 (4)	C(5')	6700 (13)	446 (3)	9689 (8)	47 (5)
O(1')	6777 (11)	2149 (3)	8854 (7)	79 (5)	C(6')	4686 (13)	153 (3)	8514 (8)	50 (5)
O(2')	4259 (10)	1481 (3)	10285 (5)	71 (4)	C(7')	8173 (12)	654 (3)	8350 (7)	45 (5)
O(3')	8530 (9)	1149 (3)	10241 (5)	63 (4)	C(8')	5946 (13)	438 (4)	7109 (8)	47 (5)
O(4')	3281 (13)	602 (3)	10218 (7)	96 (6)	C(9')	7320 (14)	1103 (4)	6991 (7)	47 (5)
O(5')	7634 (11)	331 (3)	10112 (7)	86 (5)	C(10')	2036 (13)	1333 (3)	6301 (7)	43 (5)
O(6')	4494 (10)	-139 (3)	8275 (7)	77 (5)	C(11')	4561 (14)	1198 (4)	5850 (7)	48 (5)
O(7')	9182 (10)	542 (3)	8696 (7)	76 (4)	C(12')	3015 (13)	657 (3)	6667 (7)	41 (4)
O(8')	5738 (10)	179 (3)	6740 (6)	73 (4)	C(13')	4593 (12)	1669 (3)	7327 (6)	32 (4)
O(9')	7919 (12)	1252 (4)	6600 (7)	95 (6)	C(14')	4021 (11)	1473 (3)	7922 (6)	26 (3)
O(10')	935 (9)	1417 (3)	5979 (6)	67 (4)	C(21')	5169 (6)	2238 (2)	6735 (5)	40 (4)
O(11')	5037 (11)	1249 (3)	5315 (5)	73 (4)	C(22')	4841	2570	6339	51 (5)
O(12')	2516 (11)	388 (3)	6604 (7)	75 (5)	C(23')	3458	2692	6163	55 (6)
C(1)	1568 (13)	1225 (4)	1469 (7)	42 (5)	C(24')	2404	2484	6384	44 (5)
C(2)	3346 (12)	1016 (3)	2997 (8)	46 (5)	C(25')	2732	2153	6779	34 (4)
C(3)	1980 (12)	497 (3)	2017 (8)	44 (5)	C(26')	4114	2030	6955	32 (4)
C(4)	3002 (14)	526 (4)	4388 (8)	53 (5)	C(31')	2869 (7)	1948 (2)	8618 (4)	37 (4)
C(5)	1072 (12)	83 (3)	3427 (7)	42 (4)	C(32')	1820	2063	9004	48 (5)
C(6)	179 (15)	454 (4)	4653 (8)	58 (6)	C(33')	679	1836	9026	55 (6)
C(7)	-1248 (13)	234 (4)	2141 (8)	47 (5)	C(34')	588	1494	8661	51 (5)
C(8)	-2477 (13)	553 (3)	3319 (8)	46 (5)	C(35')	1638	1379	8274	42 (4)
C(9)	-2819 (13)	880 (3)	1801 (7)	44 (5)	C(36')	2778	1606	8252	27 (4)

^a Equivalent isotropic U defined as one-third of the trace of the orthogonalized U_{ij} tensor.

a B-C single bond²¹ but lies within a range observed in carborane cages.²² The distance of 2.387 (11) Å for Ru(1)-C(14) is also longer than expected for a σ -bond (sum of covalent radii 2.01 Å); this point will be addressed in the description of the electronic structure of 1.

Each ruthenium atom in 1 carries three terminal carbonyl ligands which are unexceptional. Within the tri-ruthenium triangle, one edge is longer than the other two: Ru(1)-Ru(2) = 2.794 (1), Ru(1)-Ru(3) = 2.922 (1), and Ru(2)-Ru(3) = 2.807 (1) Å. This, considered with the orientation of the carbonyl ligands on atoms Ru(1) and Ru(3), suggests that a hydride ligand bridges the edge Ru(1)-Ru(3). This would be reasonably sited at the point of intersection of vectors O(2)C(2)Ru(1) and O(8)C(8)-Ru(3); this location is consistent with the resonance at δ -19.06 in the ¹H NMR spectrum of 1.

The spiked triangular cluster network should have a valence electron count of 64, and in order to attain this, a further cluster hydride is required. The broad ¹H NMR spectral signal at δ -7.3 implies the presence of an Ru-H-B bridging interaction. The geometry of the ligands at each

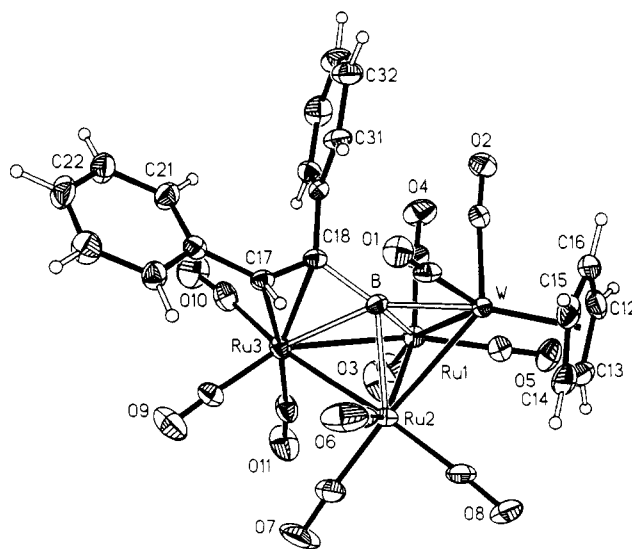


Figure 5. Molecular structure of $\text{H}(\text{CpW})\text{Ru}_3(\text{CO})_{11}\text{BC}(\text{Ph})\text{CPhH}$, 2. The cluster hydrogen atom was not located.

ruthenium atom suggests one suitable site for this hydrogen atom, viz. along the edge Ru(2)-B(1) such that the Ru(2)-H vector is approximately coincident with the O-(5)C(5)Ru(2) vector.

(21) Olmstead, M. M.; Power, P. P.; Weese, K. J. *J. Am. Chem. Soc.* 1987, 109, 2541 and references therein.

(22) Beaudet, R. A. In *Advances in Boron and the Boranes*; ed. Liebman, J. F., Greenberg, A., Williams, R. E., Eds.; VCH: New York, 1988; Chapter 20.

Table III. Selected Bond Distances and Angles for the Two Independent Molecules of 1

(a) Bond Distances/Å		
	molecule A	molecule B
Ru(1)–Ru(2)	2.794 (1)	2.786 (1)
Ru(1)–Ru(3)	2.922 (1)	2.932 (1)
Ru(1)–B	2.236 (14)	2.249 (12)
Ru(1)–C(14)	2.387 (11)	2.412 (9)
Ru(2)–Ru(3)	2.807 (11)	2.823 (2)
Ru(2)–B(1)	2.178 (13)	2.188 (12)
Ru(3)–Ru(4)	2.950 (1)	2.960 (1)
Ru(3)–B(1)	2.193 (12)	2.191 (13)
Ru(4)–B(1)	2.152 (13)	2.138 (13)
Ru(4)–C(13)	2.179 (11)	2.184 (10)
Ru(4)–C(14)	2.253 (12)	2.234 (10)
B(1)–C(14)	1.612 (17)	1.637 (16)
C(13)–C(14)	1.466 (14)	1.449 (16)
(b) Bond Angles/deg		
	molecule A	molecule B
Ru(2)–Ru(1)–Ru(3)	58.8 (1)	59.1 (1)
Ru(2)–Ru(1)–B(1)	49.8 (3)	50.1 (3)
Ru(3)–Ru(1)–B(1)	48.1 (3)	47.8 (3)
Ru(2)–Ru(1)–C(14)	87.6 (3)	88.1 (2)
Ru(3)–Ru(1)–C(14)	76.6 (3)	76.6 (3)
B(1)–Ru(1)–C(14)	40.6 (4)	40.9 (4)
Ru(1)–Ru(2)–Ru(3)	62.9 (1)	63.0 (1)
Ru(1)–Ru(2)–B(1)	51.7 (4)	52.1 (3)
Ru(3)–Ru(2)–B(1)	50.3 (3)	49.9 (4)
Ru(1)–Ru(3)–Ru(2)	58.3 (1)	57.9 (1)
Ru(1)–Ru(3)–Ru(4)	86.1 (1)	85.6 (1)
Ru(2)–Ru(3)–Ru(4)	91.3 (1)	91.2 (1)
Ru(1)–Ru(3)–B(1)	49.3 (4)	49.5 (3)
Ru(2)–Ru(3)–B(1)	49.8 (3)	49.8 (3)
Ru(4)–Ru(3)–B(1)	46.7 (3)	46.1 (3)
Ru(3)–Ru(4)–B(1)	47.8 (3)	47.6 (4)
Ru(3)–Ru(4)–C(13)	84.4 (3)	84.0 (3)
B(1)–Ru(4)–C(13)	74.2 (4)	74.3 (4)
Ru(3)–Ru(4)–C(14)	77.9 (3)	78.6 (3)
B(1)–Ru(4)–C(14)	42.9 (4)	43.9 (4)
C(13)–Ru(4)–C(14)	38.6 (4)	38.3 (4)
Ru(1)–B(1)–Ru(2)	78.5 (4)	77.8 (4)
Ru(1)–B(1)–Ru(3)	82.6 (4)	82.6 (4)
Ru(2)–B(1)–Ru(3)	79.9 (4)	80.3 (4)
Ru(1)–B(1)–Ru(4)	131.9 (6)	131.8 (6)
Ru(2)–B(1)–Ru(4)	144.1 (7)	145.6 (6)
Ru(3)–B(1)–Ru(4)	85.5 (4)	86.3 (5)
Ru(1)–B(1)–C(14)	74.7 (7)	74.9 (6)
Ru(2)–B(1)–C(14)	143.1 (8)	142.3 (9)
Ru(3)–B(1)–C(14)	120.5 (7)	120.8 (8)
Ru(4)–B(1)–C(14)	71.9 (6)	71.2 (6)
Ru(1)–C(14)–Ru(4)	119.4 (4)	119.0 (4)
Ru(1)–C(14)–B(1)	64.6 (6)	64.2 (5)
Ru(4)–C(14)–B(1)	65.2 (6)	64.9 (6)
Ru(1)–C(14)–C(13)	107.5 (7)	106.2 (7)
Ru(4)–C(14)–C(13)	68.0 (6)	69.0 (6)
B(1)–C(14)–C(13)	116.0 (9)	115.4 (10)

Molecular Structure of 2. The molecular structure of compound **2** is shown in Figure 5, and selected bond distances and angles are listed in Table V. In contrast to **1**, the tetrametal core in **2** retains the butterfly framework present in the starting material and the structure of **2** is reminiscent of that observed for the carbido-derivative $\text{HRu}_4(\text{CO})_{12}\text{CC}(\text{Ph})\text{CPhH}^2$ (Figure 1b).

Two characteristic parameters of the butterfly, viz. the internal dihedral angle (α) and the height of the interstitial atom above the wing tip-wing tip vector (h), are significantly altered in going from $\text{H}(\text{CpW})\text{Ru}_3(\text{CO})_{11}\text{BH}$ to **2**. In $\text{H}(\text{CpW})\text{Ru}_3(\text{CO})_{11}\text{BH}$, $\alpha = 111.0^\circ$ ⁸ and $h = 0.36 \text{ \AA}$ ²³ compared to values of 120.1° and 0.51 \AA in **2**. The two parameters are mutually dependent if the boron atom is to remain within effective bonding distance of each metal

Table IV. Atomic Coordinates ($\times 10^4$) and Isotropic Thermal Parameters ($\text{\AA}^2 \times 10^3$) for **2**

	x	y	z	U^a
W	4484 (1)	434 (1)	7740 (1)	31 (1)
Ru(1)	6562 (1)	1127 (1)	8365 (1)	35 (1)
Ru(2)	5528 (1)	1179 (1)	6591 (1)	35 (1)
Ru(3)	6231 (1)	2957 (1)	7398 (1)	39 (1)
B	5096 (6)	1855 (6)	7686 (6)	32 (3)
O(1)	2810 (4)	1871 (5)	6937 (4)	52 (2)
O(2)	4436 (6)	1083 (5)	9521 (4)	62 (3)
O(3)	8787 (6)	1305 (8)	8934 (7)	106 (5)
O(4)	6719 (6)	1669 (6)	10165 (4)	74 (3)
O(5)	6790 (5)	-948 (5)	8922 (5)	65 (3)
O(6)	3592 (6)	1781 (7)	5307 (4)	80 (3)
O(7)	6700 (7)	1726 (7)	5419 (5)	97 (4)
O(8)	5489 (7)	-878 (6)	5967 (5)	77 (4)
O(9)	5819 (6)	4031 (7)	5734 (5)	83 (4)
O(10)	7135 (7)	4668 (6)	8512 (6)	94 (4)
O(11)	8239 (5)	2415 (6)	7323 (6)	81 (4)
C(1)	3461 (6)	1386 (6)	7251 (5)	39 (3)
C(2)	4473 (7)	891 (6)	8861 (6)	44 (3)
C(3)	7969 (7)	1266 (8)	8692 (7)	59 (4)
C(4)	6616 (7)	1506 (7)	9479 (6)	48 (3)
C(5)	6618 (7)	-187 (7)	8658 (6)	46 (3)
C(6)	4320 (8)	1561 (8)	5789 (6)	54 (4)
C(7)	6280 (8)	1548 (8)	5876 (7)	59 (4)
C(8)	5471 (7)	-97 (8)	6211 (6)	51 (4)
C(9)	5965 (7)	3655 (7)	6347 (7)	54 (4)
C(10)	6778 (8)	4033 (8)	8120 (7)	59 (4)
C(11)	7490 (7)	2561 (7)	7371 (7)	53 (4)
C(12)	4459 (8)	-1105 (7)	8285 (6)	56 (4)
C(13)	4696 (7)	-1212 (7)	7505 (6)	51 (4)
C(14)	3866 (7)	-897 (7)	6836 (7)	54 (4)
C(15)	3124 (7)	-590 (6)	7177 (7)	54 (4)
C(16)	3483 (8)	-730 (7)	8051 (7)	59 (5)
C(17)	4518 (5)	3489 (6)	7109 (5)	33 (3)
C(18)	4850 (5)	2908 (6)	7816 (5)	32 (3)
C(21)	4456 (8)	5181 (7)	7668 (6)	50 (4)
C(22)	4146 (8)	6128 (7)	7521 (6)	57 (4)
C(23)	3605 (7)	6402 (7)	6716 (7)	58 (4)
C(24)	3392 (8)	5778 (8)	6042 (6)	59 (4)
C(25)	3707 (7)	4834 (6)	6199 (6)	44 (3)
C(26)	4223 (6)	4519 (6)	7017 (5)	36 (3)
C(31)	3837 (6)	3187 (6)	8738 (5)	43 (3)
C(32)	3687 (7)	3386 (7)	9514 (6)	56 (4)
C(33)	4466 (8)	3637 (8)	10209 (6)	61 (4)
C(34)	5398 (8)	3667 (7)	10124 (6)	59 (4)
C(35)	5554 (7)	3461 (7)	9370 (5)	45 (3)
C(36)	4778 (6)	3212 (5)	8655 (5)	34 (3)

^a Equivalent isotropic U defined as one-third of the trace of the orthogonalized U_{ij} tensor.

atom, and the change that is observed implies that the boron atom is moving from a semiinterstitial site in $\text{H}(\text{CpW})\text{Ru}_3(\text{CO})_{11}\text{BH}^8$ toward a vertex position in **2**.^{24,25} For the boron atom to be considered a cluster vertex, it should carry an exo substituent, and indeed the distance B–C(18) of 1.545 (12) Å appears to be consistent with the formation of a boron–carbon single bond^{6,21} between the alkyne and the cluster boron atom. In the organic fragment, the two phenyl groups are mutually cis. The olefinic carbon–carbon bond C(17)–C(18) is 1.382 (10) Å; this represents significant double-bond character and compares with 1.402 (5) Å in $\text{HRu}_4(\text{CO})_{12}\text{CC}(\text{Ph})\text{CPhH}^2$ and 1.466 (14) Å in **1**. Aspects of bonding will be discussed in the following section.

The Ru_3 triangle of the butterfly core of **2** is distorted with Ru(1)–Ru(3) being longer than Ru(2)–Ru(3): 2.978 (1) vs 2.853 (1) Å. In the parent compound $\text{H}(\text{CpW})\text{Ru}_3(\text{CO})_{11}\text{BH}$, the corresponding distances are 2.833 (5)

(24) Harris, S.; Bradley, J. S. *Organometallics* 1984, 3, 1086.

(25) Meng, X.; Rath, N. P.; Fehlner, T. P.; Rheingold, A. L. *Organometallics* 1991, 10, 1986.

(23) Calculated from the coordinates for $\text{H}(\text{CpW})\text{Ru}_3(\text{CO})_{11}\text{BH}^8$.

Table V. Selected Bond Distances and Angles for 2

(a) Bond Distances/Å			
Ru(1)-W	2.986 (1)	Ru(2)-W	2.961 (1)
W-B	2.185 (9)	Ru(1)-Ru(2)	2.851 (1)
Ru(1)-Ru(3)	2.978 (1)	Ru(1)-B	2.284 (8)
Ru(2)-Ru(3)	2.853 (1)	Ru(2)-B	2.302 (10)
Ru(3)-B	2.395 (10)	Ru(3)-C(17)	2.462 (8)
Ru(3)-C(18)	2.296 (9)	B-C(18)	1.545 (12)
C(17)-C(18)	1.382 (10)	C(17)-C(26)	1.495 (11)
C(18)-C(36)	1.493 (12)		
(b) Bond Angles/deg			
Ru(1)-W-Ru(2)	57.3 (1)	Ru(1)-W-B	49.5 (2)
Ru(2)-W-B	50.4 (3)	W-Ru(1)-Ru(2)	60.9 (1)
W-Ru(1)-Ru(3)	96.9 (1)	Ru(2)-Ru(1)-Ru(3)	58.6 (1)
W-Ru(1)-B	46.7 (2)	Ru(2)-Ru(1)-B	51.9 (2)
Ru(3)-Ru(1)-B	52.1 (2)	W-Ru(2)-Ru(1)	61.8 (1)
Ru(1)-Ru(2)-Ru(3)	63.0 (1)	Ru(1)-Ru(2)-B	51.3 (2)
W-Ru(2)-B	47.0 (2)	Ru(3)-Ru(2)-B	54.1 (2)
Ru(1)-Ru(3)-Ru(2)	58.5 (1)	Ru(1)-Ru(3)-B	48.8 (2)
Ru(2)-Ru(3)-B	51.1 (2)	W-B-Ru(1)	83.8 (3)
W-B-Ru(2)	82.5 (3)	W-B-Ru(3)	154.1 (5)
W-B-C(18)	138.5 (7)	Ru(1)-B-Ru(2)	76.9 (3)
Ru(1)-B-Ru(3)	79.0 (3)	Ru(2)-B-Ru(3)	74.8 (3)
W-B-C(18)	138.5 (7)	Ru(1)-B-C(18)	124.8 (5)
Ru(2)-B-C(18)	129.2 (6)	Ru(3)-B-C(18)	67.3 (5)
Ru(3)-C(17)-C(18)	66.6 (4)	C(18)-C(17)-C(26)	131.5 (7)
Ru(3)-C(18)-B	74.3 (5)	Ru(3)-C(18)-C(17)	79.8 (5)
B-C(18)-C(17)	118.3 (7)	B-C(18)-C(36)	119.2 (7)
Ru(3)-C(18)-C(36)	126.6 (5)	C(17)-C(18)-C(36)	121.3 (7)
Cp(centroid)-W-Ru(1)	131.0 (1)	Cp(centroid)-W-Ru(2)	119.7 (1)
Cp(centroid)-W-B	169.6 (3)	Cp(centroid)-W-C(1)	111.2 (3)
Cp(centroid)-W-C(2)	108.0 (3)	W-C(1)-O(1)	173.7 (7)
W-C(2)-O(2)	174.3 (8)		

and 2.825 (5) Å.⁸ However, the lengthening of one Ru_{wing}-Ru_{hinge} edge in 2 falls far short of that needed to cause the bond cleavage observed in 1.

In 2, the boron atom to hinge-ruthenium and tungsten distances of 2.284 (8), 2.302 (10), and 2.185 (9) Å, respectively are similar to those in H(CpW)Ru₃(CO)₁₁BH (2.27 (7), 2.32 (7), and 2.21 (6) Å) but the introduction of the organic fragment results in significant lengthening of Ru_{wing tip}-B from 2.04 (6) Å in H(CpW)Ru₃(CO)₁₁BH to 2.395 (10) Å in 2. Compare this to the case described above for 1.

Each ruthenium atom bears three terminal carbonyl ligands, and the orientations of those attached to atoms Ru(1) and Ru(2) are consistent with the placement of a bridging hydride ligand along Ru(1)-Ru(2). In support of this, we observe that the length of Ru(1)-Ru(2) is little changed in going from H(CpW)Ru₃(CO)₁₁BH (2.841 (6) Å) to 2 (2.851 (1) Å) implying that the hydride ligand bridging this edge in H(CpW)Ru₃(CO)₁₁BH is still present in 2.

For the two carbonyl ligands attached to the tungsten atom the W-C-O angles are ≈174° and the CpW environment is that of a simple piano stool. The distance from the tungsten atom to the centroid of the Cp ring is 2.023 (1) Å.

Electronic Structures of 1 and 2. The Fenske-Hall quantum chemical method has been used to investigate the different modes of bonding between the boron-containing tetrametal fragment and the [PhHCCPh] unit in compounds 1 and 2. For this purpose the model compounds HRu₄(CO)₁₂BHC(H)CH₂ (1') and H(CpMo)Ru₃(CO)₁₁BC(H)CH₂ (2') have been used (see Experimental Section).

The [C₂H₃]⁺ fragments in both 1' and 2' are geometrically similar, derived from ethene with substituents bent back and a vacant coordination site on one carbon atom. The frontier orbitals of the fragment are shown in Figure 6 and may conveniently be labeled as σ (MO 6), π (MO 5), and π* (MO 7). Of 1 and 2, compound 2 appears to have the simpler molecular structure, and we shall address the bonding in this cluster first.

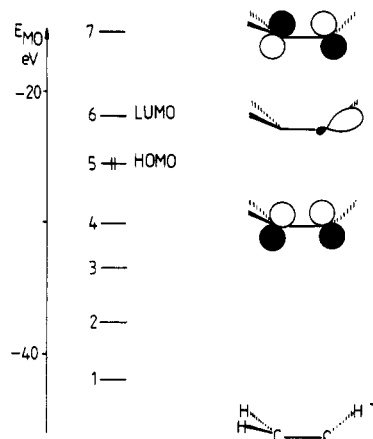


Figure 6. MO diagram for the [C₂H₃]⁺ fragment from 1', showing the three frontier orbitals. A corresponding diagram for the fragment from 2' is similar.

Table VI. Mulliken Overlap Populations (MOP) between the MOs of Fragments [H(CpMo)Ru₃(CO)₁₁B]⁻ and [C₂H₃]⁺ To Generate 2'

fragment MOs for [H(CpMo)Ru ₃ (CO) ₁₁ B] ⁻	fragment MOs for [C ₂ H ₃] ⁺		
	5 (HOMO)	6 (LUMO)	7
83	0.023	0.056	
84	0.012	0.019	0.030
85 (HOMO)	0.071	0.037	0.016
86 (LUMO)			
87	0.027	0.058	
88	0.012	0.044	
tot. MOP per MO of [C ₂ H ₃] ⁺ (as % of tot. MOP)	0.145 (36)	0.214 (53)	0.046 (11)

The LUMO, MO 86, of [H(CpMo)Ru₃(CO)₁₁B]⁻ possesses π-antibonding character between each wing-tip metal atom and the boron atom; MO 86 is nonbonding with respect to interactions between the [H(CpMo)Ru₃(CO)₁₁B]⁻ and [C₂H₃]⁺ fragments. Frontier orbitals 83, 84, 85, 87, and 88 all possess boron character. The fact that the boron atom resides 0.5 Å above the butterfly wing tip-wing tip axis²⁶ allows boron-centered outward pointing radial orbital character to be exposed,²⁷ notably in MOs 87 and 88. This prepares the boron atom for bonding to an exo substituent.²⁶ In MO 85 (HOMO), the radial character is coupled with tangential character and permits the evolution of Ru_{wing tip}-B bonding character. Thus, the HOMO of the [H(CpMo)Ru₃(CO)₁₁B]⁻ fragment is reminiscent of the HOMO of the related butterfly anion [HF₄(CO)₁₂BH]⁻.²⁸

Interfragment Mulliken overlap populations (MOP) for the interactions of MOs 5, 6, and 7 of [C₂H₃]⁺ with the frontier MOs of the [H(CpMo)Ru₃(CO)₁₁B]⁻ fragment from 2' are listed in Table VI. The total MOP values given per MO of the organic fragment indicate the relative importance of interactions involving the σ, π, or π* MOs of [C₂H₃]⁺. Interfragment interactions (83-6), (88-6), and (85-5) are drawn schematically in Figure 7. The σ-lobe of MO 6 of [C₂H₃]⁺ is directed at the boron atom but, by virtue of the position of the organic fragment with respect to the cluster framework, interacts quite effectively with both radially and tangentially oriented boron-centered orbitals; this is apparent if one compares the MOPs for

(26) Raising the main group atom E above the wing tip-wing tip axis effectively alters the cluster description from arachno (with interstitial atom E) to closo (with E being a vertex atom): see refs 24, 27, and 28.

(27) Housecroft, C. E. *J. Organomet. Chem.* 1984, 276, 297.

(28) Fehner, T. P.; Housecroft, C. E.; Scheidt, W. R.; Wong, K. S. *Organometallics* 1983, 2, 825.

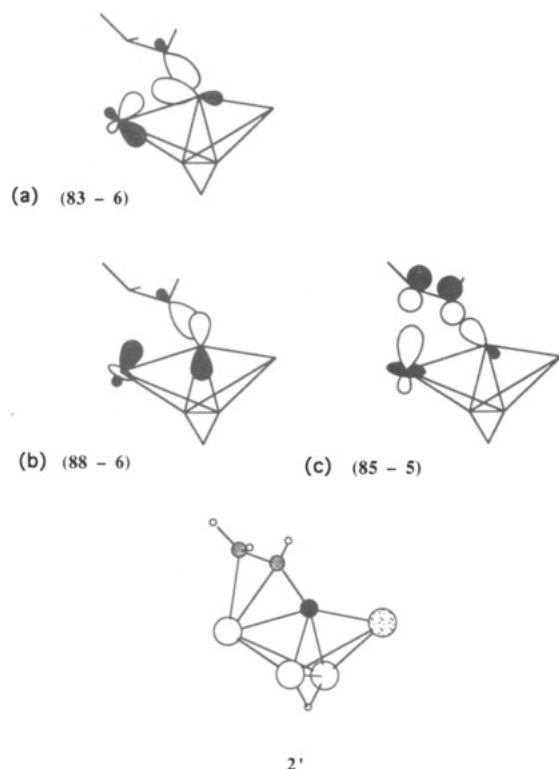


Figure 7. Schematic representations of $[\text{H}(\text{CpMo})\text{Ru}_3(\text{CO})_{11}\text{B}]^-$ - $[\text{C}_2\text{H}_3]^+$ interfragment interactions (a) (83-6), (b) (88-6), and (c) (85-5) in $2'$.

the "radial interactions" (87-6) and (88-6), the "tangential interaction" (83-6), and the interaction (85-6), which contains both boron radial and tangential components. Thus, although tending toward an exo-B-C bond, B-C(18) (see Figure 5) does retain some endo character.

Orbitals 5 and 7 of the $[\text{C}_2\text{H}_3]^+$ fragment are involved primarily in π -interactions with the wing-tip ruthenium atom. The total MOP values listed in Table VI indicate that π -donation significantly outweighs π -back-donation.²⁹ The principal π -interaction is shown schematically in Figure 7c; note that this interfragment interaction does involve some boron character and is not simply a localized alkene \rightarrow metal π -bond.

In $1'$, the $[\text{C}_2\text{H}_3]^+$ fragment lies over the cavity which is exposed once the Ru_4B -butterfly skeleton has opened-up. The frontier MOs 75, 76, 77, and 79 of the spiked triangular $[\text{HRu}_4(\text{CO})_{12}\text{BH}]^-$ fragment all possess significant boron atom character; MO 78 possesses Ru(1), Ru(2), and Ru(3) orbital character and MO 80 is an outward pointing sp²-hybrid lobe localized on the "spike" atom Ru(4) (see Figure 4). Interfragment MOPs for the orbital interactions of $[\text{HRu}_4(\text{CO})_{12}\text{BH}]^-$ with $[\text{C}_2\text{H}_3]^+$ to generate $1'$ are listed in Table VII; the final totals and percentages indicate the relative roles of the σ -, π -, and π^* -orbitals of the organic fragment. Important interactions are shown in Figure 8.

MO 6 of the $[\text{C}_2\text{H}_3]^+$ fragment is localized on carbon atom C(14) and is directed at a point between atoms B(1) and Ru(1) (see Figure 4 for atom numbering). A total of 17% of the overall interfragment bonding arises from the interaction (79-6) (Figure 8a). This interaction gives rise to a 3-center-2-electron bridge involving atoms C(14), B(1), and Ru(1). In addition, a 3-center bond is produced as a consequence of interaction (79-7) (Figure 8c); (79-7) constitutes 11% of the total interfragment bonding. In-

Table VII. Mulliken Overlap Populations (MOP) between the MOs of Fragments $[\text{HRu}_4(\text{CO})_{12}\text{BH}]^-$ and $[\text{C}_2\text{H}_3]^+$ to generate $1'$

fragment MOs for $[\text{HRu}_4(\text{CO})_{12}\text{BH}]^-$	fragment MOs for $[\text{C}_2\text{H}_3]^+$		
	5 (HOMO)	6 (LUMO)	7
65		0.024	
75		0.026	0.039
76		0.043	
77		0.028	0.030
78			0.019
79 (HOMO)		0.092	0.060
80 (LUMO)	0.160	0.036	
tot. MOP per MO of $[\text{C}_2\text{H}_3]^+$ (as % of tot. MOP)	0.160 (29)	0.249 (45)	0.148 (26)

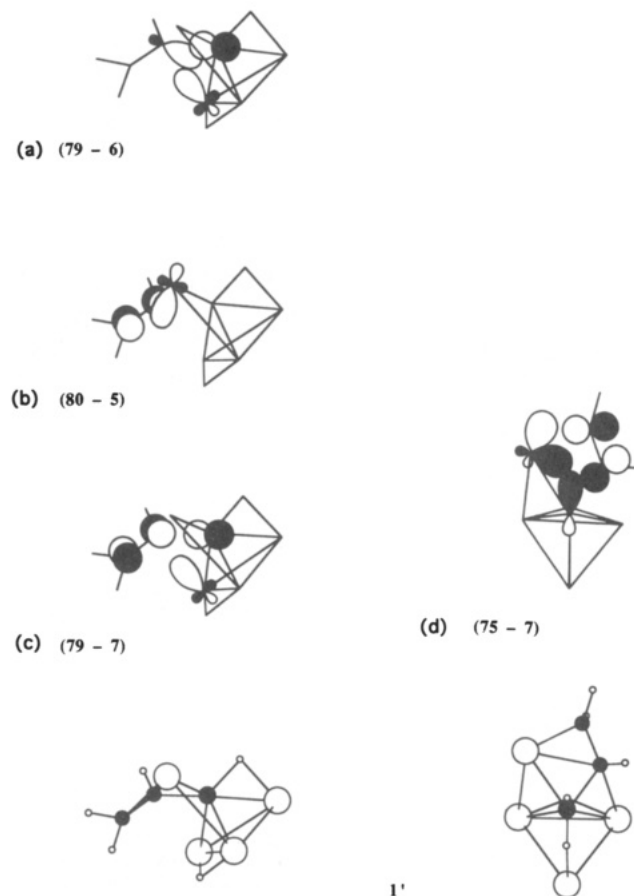


Figure 8. Schematic representations of $[\text{HRu}_4(\text{CO})_{12}\text{BH}]^-$ - $[\text{C}_2\text{H}_3]^+$ interfragment interactions (a) (79-6), (b) (80-5), (c) (79-7), and (d) (75-7) in $1'$.

teractions (79-6) and (79-7) are the major factors which cause the observed lengthening of edges B(1)-C(14) and Ru(1)-C(14).²⁹

The interaction of the "spike" atom Ru(4) with the organic fragment is essentially as expected; interaction (80-5) is a localized alkene \rightarrow metal π -donation (Figure 8b) and interactions (75-7) and (78-7) constitute the π -back-donation. However, in (75-7) (Figure 8d) significant boron atom character intrudes upon the Dewar-Chart-Duncanson model enhancing the B(1)-C(14) bond and giving rise to some degree of Ru(4)-B(1)-C(14) bridge-bonding character. Inspection of Tables VI and VII initially leads one to believe that the degree of back-bonding in $1'$ (and thus 1) is greater than in $2'$ (or 2). However, as Figure 8c illustrates, the involvement of the π^* orbital of the $[\text{C}_2\text{H}_3]^+$ fragment in interaction (79-7) enhances the B(1)-C(14)-Ru(1) 3-center interaction and has no bearing on the back-donation from Ru(4) to the organic fragment. The

(29) Bond lengths used in the calculation clearly influence actual MOP values, but we seek a qualitative picture of the bonding in compounds $1'$ and $2'$.

same is true for interaction (77-7). Thus, as in 2', π -donation dominates over π -back-donation.

Electron Counting in 1 and 2 Revisited. The experimentally determined molecular structures of 1 and 2 lead to the descriptions of 64-electron spiked triangular and 62-electron butterfly clusters, respectively.^{30,31} For 1, we may consider the $\text{Ru}_4(\text{CO})_{12}$ skeleton as providing 56, the boron atom 3, two endo-hydrogen atoms 1 each, and the CPhCHPh unit 1 σ - and 2 π -electrons, making a total of 64 electrons. From 1 to 2, the observed increase in dihedral angle, α , and height, h , of the boron atom above the wing tip-wing tip vector led us in the discussion of the molecular structure of 2 to conclude that the boron atom was no longer interstitial. Thus an appropriate electron count would be 57 from the $\text{CpWRu}_3(\text{CO})_{11}$ skeleton, 1 from the cluster hydride ligand, 2 from the olefinic π -interaction, and 2 from the exo-BR (R = CPhCHPh) unit, making a total of 62 electrons. While these electron distributions clearly "work" in terms of the effective atomic number rule,^{30,31} the results of the Fenske-Hall calculations imply that in both compounds there is a degree of ambiguity concerning any simple (e.g. exo versus interstitial character for the boron atom and Dewar-Chart-Duncanson model for the ruthenium-alkene bonding) bonding scheme which may be used to describe the two molecules.

Conclusions. The reaction of $\text{HRu}_4(\text{CO})_{12}\text{BH}_4$ with $\text{PhC}\equiv\text{CPh}$ leads to an unprecedented cluster by virtue of concomitant B-C bond formation, transfer of a cluster-bound hydrogen atom to the alkyne, and insertion of the

organic unit into the Ru_4 butterfly to yield a spiked triangular framework retaining a μ_4 -boron atom. In contrast, the reaction of $\text{PhC}\equiv\text{CPh}$ with $\text{H}(\text{CpW})\text{Ru}_3(\text{CO})_{11}\text{BH}$ proceeds with retention of the butterfly skeleton although, as in the first reaction, cluster-to-alkyne hydrogen atom transfer occurs along with B-C bond formation. Both reactions involve the formation of an alkene-ruthenium π -bond.

The reason(s) for the differences in reaction pathways are not as yet clear to us. One possibility is that the presence of the additional B-H-Ru hydrogen atom in 1 inhibits the boron atom from moving out of the butterfly framework as is required in the formation of 2. However, other work in progress in our laboratory indicates that in some cases a small unsaturated molecule may be incorporated into $\text{HRu}_4(\text{CO})_{12}\text{BH}_2$ without cluster opening.³²

Acknowledgments are made to the donors of the Petroleum Research Fund, administered by the American Chemical Society, for support of this work (Grants No. 19155-AC3 and No. 22771-AC3), to the SERC for studentships (to D.M.M. and J.S.H.), and to the NSF for a grant (CHE 9007852) toward the purchase of a diffractometer at the University of Delaware. Johnson-Matthey is thanked for generous loans of RuCl_3 .

Supplementary Material Available: Tables of positional and thermal parameters and bond distances and angles (15 pages). Ordering information is given on any current masthead page.

OM9204200

(30) Mingos, D. M. P. *Nature (London) Phys. Sci.* 1972, 236, 99.

(31) Lauher, J. W. *J. Am. Chem. Soc.* 1978, 100, 5305.

(32) Housecroft, C. E., Song, X. Manuscript in preparation.

Determination of the Free Activation Energies for the Interconversion of Isomers of 2,4-Pentadienyldipropylborane via Consecutive 1,3-Boron Shifts

Mikhail E. Gurskil, Ilya D. Gridnev, Alexei V. Geiderikh, Anatoly V. Ignatenko, and Yuri N. Bubnov*

N. D. Zelinsky Institute of Organic Chemistry of the Russian Academy of Sciences, Leninsky prosp., 47, Moscow B-334, 117913 Russia

Vadim I. Mstislavsky and Yuri A. Ustynyuk*

Chemistry Department of Moscow State University, Moscow, 117234 Russia

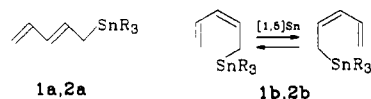
Received April 10, 1992

The fluxional behavior of the *E* (4a) and *Z* (4b) isomers of 2,4-pentadienyldipropylborane has been studied by dynamic ^1H and ^{13}C NMR spectroscopy. Activation barriers have been determined for degenerate metallotropic rearrangements of 4a and 4b and for 4a \rightleftharpoons 4b interconversion by complete line shape analysis of ^{13}C DNMR spectra. The data obtained suggest that only 1,3 shifts of BPr_2 groups take place in both isomers rather than 1,5 sigmatropic shifts.

Introduction

The chemistry of the 2,4-pentadienyl organometallic compounds has been extensively investigated.¹ Pentadienyl derivatives of alkali metals (Na, K, Rb, Cs) are ionic and fluxional in solution due to the rapid equilibration of S-, W-, and U-conformers of the pentadienyl anion.²⁻⁴

Scheme I



1b R=Ph, ΔG^\ddagger 81 kJ/mol [9]
2b R=Cl, ΔG^\ddagger < 30 kJ/mol [10]

(1) For a review, see: (a) Yasuda, H.; Nakamura, A. *J. Organomet. Chem.* 1985, 285, 15-29. (b) Ernst, R. D. *Acc. Chem. Res.* 1985, 18, 56-62.

Pentadienyl compounds of lithium,⁵ magnesium,⁶ beryllium,⁷ and zinc⁷ demonstrate more complex fluxionality